EUROPHYSICS LETTERS 15 June 2004

Europhys. Lett., **66** (6), pp. 812–818 (2004)
DOI: 10.1209/epl/i2003-10266-0

Pattern formation without heating in an evaporative convection experiment

H. Mancini(*) and D. Maza

Departamento de Física y Matemática Aplicada, Facultad de Ciencias Universidad de Navarra - 31080 Pamplona, Spain

(received 12 November 2003; accepted in final form 19 April 2004)

PACS. 47.54.+r – Pattern selection; pattern formation.
PACS. 47.20.Dr – Surface-tension-driven instability.
PACS. 47.20.Hw – Morphological instability; phase changes.

Abstract. – We present an evaporation experiment in a single fluid layer reproducing conditions of volatile fluids in nature. When latent heat associated to the evaporation is large enough, the heat flow through the free surface of the layer generates temperature gradients that can destabilize the conductive motionless state giving rise to convective cellular structures without any external heating. Convective cells can be then observed in the transient range of evaporation from an initial depth value to a minimum threshold depth, after which a conductive motionless state appears until the evaporation finishes with an unwetting sequence. The sequence of convective patterns obtained here without heating is similar to that obtained in Bénard-Marangoni convection. This work presents the sequence of spatial bifurcations as a function of the layer depth. The transition between square-to-hexagonal pattern, known from non-evaporative experiments, is obtained here with a similar change in wavelength.

Introduction. – Pattern formation in different areas of knowledge has received great attention in the last decade [1,2]. Interest in this kind of research arises from the general interest in understanding nature and also from requirements of industrial processes like painting, film drying or crystal growth, where pattern formation knowledge plays a fundamental role. Pattern formation during evaporation is a common phenomena that can be frequently observed in nature. Natural convection self-generated by the evaporation of a thin layer of water normally leaves the brand of its individual convective cells in the bottom clay.

Since the first rigorous work devoted to study pattern formation in fluids [3], the existence of cellular structures was recognized to be linked to surface tension and buoyancy. Experimental and theoretical studies where movements are generated mostly by interfacial forces [4, 5] have increased in the last years [6, 7]. Generally, convective movements originated in surface tension gradients are known as Marangoni or Bénard-Marangoni (BM) convection. In evaporative convection there are two main physical mechanisms of instability relating surface tension

(*) E-mail: hmancini@fisica.unav.es

gradients, one with a change in the composition or concentration, which is called *thermosolutal convection*, and the other with the local dependence of surface tension on temperature or *thermocapillary convection*.

In the first one, experiments are normally performed using alcohols or other evaporative fluids like polymers in solution, where the proportion between solute and solvent can be changed by evaporation [8,9]. As an example, Zhang and Chao [10] presented an experimental work reporting the onset of patterns considering heating (or even cooling) and evaporation using this kind of fluids. They used a thin liquid layer of alcohol (among other liquids) heated from below and the convective structures have been observed by seeding the fluid with aluminum powder.

In pure thermocapillary convection, temperature is involved directly and movements are now related with local temperature dependence of surface tension. Hydrodynamic instabilities grow as in the Bénard original works, but, to our knowledge, previous experimental results on pattern formation in evaporation of pure fluids do not exist. Recently, Maillard *et al.* [11] presented a microscopic evidence of unusual patterns (micron-sized objects like rings and hexagonal arrays) that they consider patterns of Bénard-Marangoni convection driven by surface tension gradients. Even if the work is not performed with an evaporative fluid, it certifies that interest of material sciences in the production and control of well-ordered arrays of this kind of cells at micron scale is increasing.

Regarding the evaporation properties, there is a family of experimental and theoretical studies aiming to determine constants like the Sherwood number (the dimensionless rate of evaporation) under different conditions [12,13], or the temperature profile near the evaporating surface [14, 15]. Normally, pattern formation is not specific and it must be said that the simultaneous measurement of all parameters involved is normally a complex task.

In all the above-mentioned experiments, patterns are composed mostly by irregular cells. Normally, the aspect ratio is large (we call aspect ratio Γ, the ratio between the horizontal characteristic dimension and the depth). In the previous experiments, to our knowledge, no attempts have been made to compare evaporative experiments with theory in the frame of pattern formation. The present work is the first experiment devoted to check the convective pattern sequence appearing in an evaporation layer without heating and to compare it with non-evaporative convection.

The experiment. – It is well known from thermodynamics that equilibrium between a fluid and its vapor phase is bidimensional. The equilibrium states are all on a line in the plane defined by pressure p, and temperature T. In a closed environment with a layer of volatile fluid, the fluid evaporates until the vapor phase reaches the vapor pressure corresponding to the fluid temperature. When the equilibrium pressure is reached evaporation stops. If a part of the atmosphere composed by air plus vapor is removed (*i.e.* blowing slightly), the fluid tends to evaporate continuously until it recovers its equilibrium value. If the volume of air is replaced at the same rate that the mixture of vapor plus air is removed, a constant evaporation rate can be reached. Under these conditions, evaporation follows until all the liquid layer disappears. This a common situation in nature when the wind removes the vapor phase in equilibrium with a fluid and makes a volatile layer completely evaporate.

In the experiment here presented we reproduce these conditions introducing all the set-up in a closed box and evacuating a small part of the total volume of the inner box atmosphere. A scheme of the system can be seen in fig. 1a.

The fluid used was hexametildisiloxane ($C_6H_{18}OSi_2$) and it was chosen because it is a pure volatile fluid at atmospheric pressure (Prandtl number = 14.5). Properties of this and other silicon oils can be obtained from different handbooks [16, 17]. It was placed in a cylindrical container on a computer-controlled analytical balance in order to measure in real time the

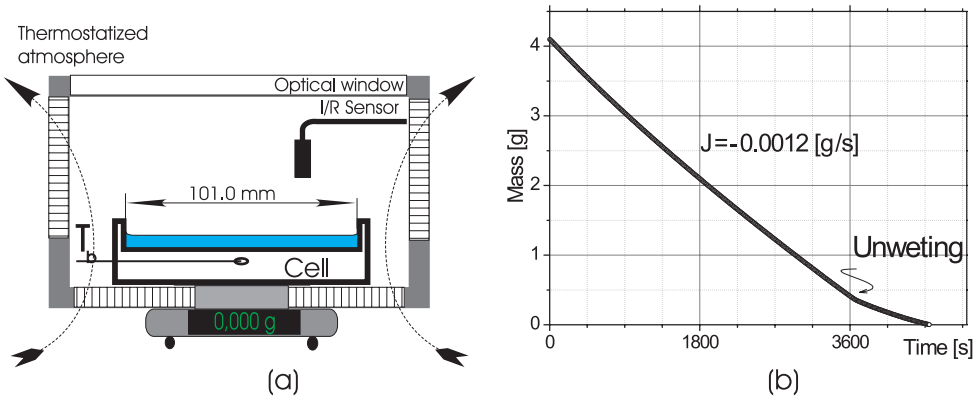

Fig. 1 – (a) Scheme of the experiment: a cylindrical cell is mounted in a closed environment, where a very small flow refreshes air and vapor pressure. An infrared sensor checks the temperature near the free surface and a thermocouple measures the temperature near the bottom of the fluid layer T_{b}. (b) The weak pressure unbalance induced by the controlled air flow drives an almost linear evaporation rate until the drying process begins.

evaporated mass (with a resolution of 0.001 g). The atmosphere inside the box, composed by the vapor pressure of the fluid plus air, was kept at a constant pressure by refilling with a laminar flow of new air at the same temperature and at the same rate of evacuation. This stationary state, slightly out of equilibrium, generates a constant rate of evaporation. The evaporation rate $\boldsymbol{J}$ is defined by the rate at which the vapor pressure is removed from the gas phase and by the equilibrium temperature of the fluid phase with the atmosphere.

There is no external heating or cooling in this experiment. The latent heat is the responsible for convection. The pool is left to reach its own thermal equilibrium with the environment in a time that depends on its thermal conductivity. Thermal exchanges are restricted to different parts of the system at the interior of the box. The box with all the system is placed in a conditioned-air room in order to keep also the external temperature constant, $T_{\mathrm{atmosphere}} = 20\,^{\circ}\mathrm{C}$. The latent heat extracted from the fluid is subsequently recovered from the surroundings of the layer. Two extreme conditions of conductivity had been used in the container of the fluid to check their influence. One was a good conductor aluminum cell and the other was a cell with equal dimensions and geometry but constructed with a thermal insulating material. We did not find significative differences in the patterns. In the experiment, patterns appear if the evaporation rate and the fluid depth are adequate. To obtain ordered patterns, the evaporation rate $\boldsymbol{J}$ must be relatively low. In a typical sequence $\boldsymbol{J}$ was controlled as $0.0010\,\mathrm{g/s} < \boldsymbol{J} < 0.0015\,\mathrm{g/s}$. Before the unwetting (or drying) process and without refilling the cell with new fluid, the depth of the layer changes linearly from a fixed and arbitrary initial value to zero, independently of what kind of patterns appear.

The depth of the liquid layer is calculated from the mass, the volume of the cylindrical container (area $= 80.12\,\mathrm{cm}^2$), and the fluid density ($0.760\,\mathrm{g/cc}$). A typical evaporation rate obtained in the experiment can be seen in fig. 1b. It is interesting to note that only when the drying process of the layer begins, does a sudden change in the evaporation rate appear.

Pattern dynamics. – Patterns are observed by usual shadowgraph techniques described in other experiments by the authors [18]. The transient sequence of patterns shown in fig. 2

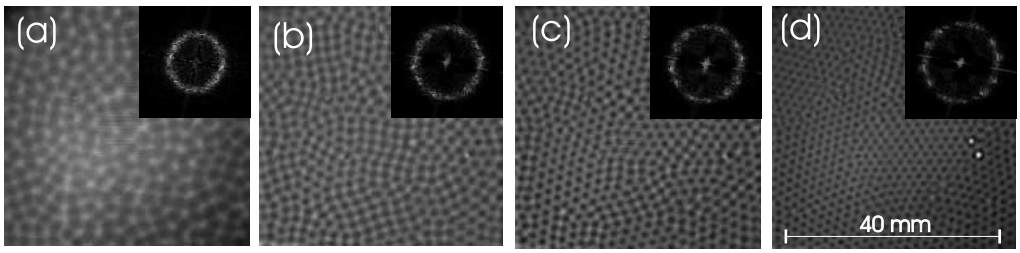

Fig. 2 – Sequence of patterns obtained as a function of decreasing depth and their FFT spectra. (a) $d = 0.8\,\mathrm{mm}$; (b) $d = 0.6\,\mathrm{mm}$; (d) $d = 0.5\,\mathrm{mm}$; (e) $d = 0.4\,\mathrm{mm}$.

has been obtained when a linear change in depth with time is performed in the experiment. We used an image processing system to capture images that are processed and stored together with the corresponding outputs of the data acquisition system. Images and data files of temperatures, depths and evaporation rates obtained at the same time are then used to obtain the results here presented. The error in time synchronism of all the system is negligible. To control the results, each experiment has been performed more than 20 times. It was verified that if the evaporated mass is refilled in the pool keeping the depth constant, a stationary pattern can be obtained. As shown in fig. 1b, the change in depth at a fixed evaporation rate fits an almost linear function. The second-order coefficient (deviation from linearity) is obtained reproducibly and is two orders of magnitude lower than the linear coefficient.

The sequence begins when the cell is filled with a fixed and arbitrary initial depth of fluid (usually we used $d_0 = 2\,\mathrm{mm}$). Considering the diameter of the cell ($D = 101\,\mathrm{mm}$), we have an initial aspect ratio of $\Gamma \approx 50$. Initially, convective movements are turbulent. Movements are mostly formed by buoyant plumes which are born at the bottom of the cell and appear randomly distributed in space and time. When the layer depth goes under a certain value, typically $d = 0.8\,\mathrm{mm}$, a pattern formed by a few irregular and large cells fills the pool. By lowering the layer depth, the size of the cells becomes smaller and consequently the number of disordered cells increases (fig. 2a). The planform changes continuously with depth to a pattern composed by tetragonal cells (fig. 2b).

If depth goes down to approximately $d = 0.5\,\mathrm{mm}$, the pattern composed by domains of tetragonal cells changes to another of hexagonal cells as in fig. 2d, that exists until a critical depth d_c is reached. When the minimum depth is reached, the entire pattern disappears until that "drying process" begins. Drying means destruction of the layer and begins when a long-wavelength instability [19, 20] appears, giving place to another different stage in the experiment. The FFT sequence displayed in the insets of fig. 2 shows the existence of a well-defined wave number but without a preferred direction in the phase plane.

Figure 3a displays a typical data file of the mean wavelength against depth in a run. Following the idea introduced by Merckt and Bestehorn [21], we calculate the supercriticality as a function of the *square* of the fluid depth $\epsilon = \frac{d^2 - d_\mathrm{c}^2}{d_\mathrm{c}^2}$ as the parameter distance from the critical depth d_c. The results obtained are in good agreement with those reported in ref. [21].

In order to compare our results with those obtained in a non-evaporative convection with heating [6], we verify the critical depth calculating d_c from the critical Marangoni number predicted by the linear theory, using $\Delta T = 0.1\,^\circ\mathrm{C}$ measured between T_b and the free surface (a value within the limit of our experimental resolution). We obtain a rough critical depth

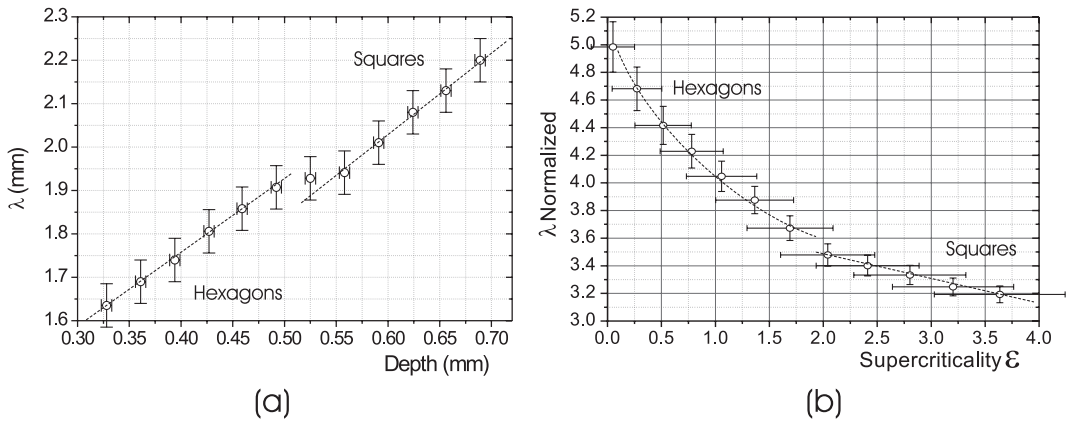

Fig. 3 – (a) Mean dimensional wavelength as a function of the liquid depth. Note the existence of a transition zone corresponding to the square-to-hexagon transition. (b) Dimensionless wave number as a function of the supercriticality. The fits are just a guide for the eye.

$d_c = 0.3\,\mathrm{mm}$. Within our optical test resolution, we measure the same critical depth $d_c = 0.3 \pm 0.02\,\mathrm{mm}$, for all the evaporation rate studied.

Experiments on the square-to-hexagon transition (SHT) have been only recently reported [19, 20]. In agreement with the results reported in ref. [20], we observed that the wave number of the pattern at the transition depended strongly on the history of the experimental sequence. In [20] the wavelength at the transition of hexagons to squares (when ϵ is increased) is 10% lower than the wavelength when the supercriticality is diminished. In our experiment, such hysteresis effect cannot be measured, but we observe a "jump" in the dimensionless wavelength when the SHT takes place (fig. 3). Note from fig. 3a that the average wavelength of the cellular pattern remains almost constant for a depth in the range $0.49\,\mathrm{mm} < d < 0.56\,\mathrm{mm}$. This fact implies approximately a jump of 5% in the wavelength normalized by the depth of the fluid. Widening this depths interval, we observed simultaneously domains of squares and hexagons as in ref. [19].

The dimensionless wave number $k_c = 1.25$ corresponding to the onset (fig. 3b), is in disagreement with the predicted value for the linear theory [22, 23] which is $k_c = 1.97$. This disagreement can be related with the fact that the convective pattern at threshold is not stationary but has a characteristic lifetime related with the evaporation rate $\boldsymbol{J}$ and the horizontal diffusion time. A more advanced experimental set-up, where the liquid depth remains almost constant during a horizontal diffusion time, has been implemented in order to study the critical wave number at the onset. These results will be reported elsewhere.

Other outputs of the experiment are the local temperatures against time (or depth). To measure local temperatures at different depths, sub-millimeter thermocouples are mounted laterally in a small hole on a plexiglass ring to avoid a pattern perturbation. Plexiglass is a thermal insulator having a similar conductivity to the silicon oil, so temperature recovering from the environment is obtained principally from the aluminum disk placed below. An infrared sensor (IR) is used to measure the temperature at the free surface. From the thermocouple put inside the cell, we determine temperature dynamics. Two regimes can be identified: a) when the flow is turbulent, the temperature difference between T_b and the atmosphere rises to a limit value between $-0.8\,^\circ\mathrm{C}$ and $-1.0\,^\circ\mathrm{C}$ and b) when the stationary pattern

stabilizes, this difference decreases to $-0.4\,^{\circ}$C and remains almost constant to the unwetting process. Finally, the temperature goes up to the initial equilibrium value. Latent heat brings the system out of thermal equilibrium. As the heat in the fluid bulk flows mainly from below, the bottom temperature is lower than the ambient temperature. But the temperature at the free surface of the fluid is even lower.

Discussion. – In this experiment a typical sequence of ordered patterns appears similar to a Bénard-Marangoni convection heated from below. As the sequence appears here without any external heating, only very few of the previously existing models describing evaporation patterns are useful. The typical cellular patterns obtained can be observed and measured reproducibly. As during the evaporation the fluid layer depth goes down, the control parameter is consequently lower and the sequence obtained is inverted with respect to the normal BM convection.

The first effect produced by evaporation in our experiment is to create the vertical temperature gradient by latent heat. So we do not need any externally imposed heating or cooling flow. The second one is to increase the thermal conductivity in the evaporating surface. This means to increase the cooling in the cold surface points and the heating in the hot surface ones. This in turn increases the effective Biot number in the models. It can be verified experimentally by observing that the system becomes strongly turbulent when the evaporating rate is increased too much. To have ordered patterns the mass flow must be controlled as in our case.

Normally, the theoretical models for this kind of experiments consider an externally imposed heating or cooling flow (from below or from above). Very recently, a theoretical work of Merkt and Bestehorn [21] appeared, where this sequence is obtained without external driving. They constructed two theoretical models, one is the two-layer (fluid and gas) approximation, where they perform a linear stability analysis. The other is a one-layer approximation with a large effective Biot number. With the second one they found that thresholds obtained in non-evaporating oils with a fixed Prandtl number fluid ($\mathrm{Pr} = 10$) are significatively lowered with increasing the Biot number. The pattern morphology is reproduced and the sequence of bifurcations obtained in our experiment is then reproduced numerically.

Conclusions. – In summary, we presented here the first experimental report of ordered spatial bifurcations produced only by evaporation and a time-resolved information of the relevant variables. The sequence of pattern described is the same as in non-evaporative convection for a control parameter increasing its value. The main features of the experiment can be explained by a recent theory [21]. We demonstrate that patterns exist in a well-defined range of depths and also that the transition between squares to hexagons appears as clearly as in non-evaporative convection, with a change in the dimensionless wave number similar to the value reported for non-evaporative convection. The tetragonal structure appears when convection is more important to the heat transport (higher depth) and this result confirms also that tetragonal cells seem to be more efficient than hexagonal ones in heat transport, as was assumed in [19].

* * *

The authors thank M. Bestehorn for sharing his theoretical results and for accepting to exchange them with the authors' experimental results before publication. The authors are also indebted to I. Zuriguel for his participation in the first stages of this experiment and to E. Mancini for the cooperation in the construction of the experimental set-up and during the development of measurements, and also thank C. Pérez García for useful discussions. This work was partially supported by the European Community network ECC TRN HPRN-CT-2000-00158 and by MCyT proyect BFM2002-02011, Spain.

REFERENCES

[1] Cross M. C. and Hohenberg P. C., *Rev. Mod. Phys.*, **65** (1993) 851.
[2] Rabinovich M., Ezersky A. and Weidman P., *The Dynamics of Patterns* (World Scientific, Singapore) 2000.
[3] Bénard H., *Rev. Gén. Sci. Pures Appl.*, **11** (1900) 1261.
[4] Block M., *Nature*, **178** (1956) 650.
[5] Scriven L. E. and Sterling C. V., *Nature*, **187** (1960) 186.
[6] Colinet P., Legros J. C. and Velarde M. G., *Nonlinear Dynamics of Surface-Tension-Driven Instabilities* (Wiley, Berlin) 2001.
[7] Nepomnyashchy A., Velarde M. G. and Colinet P., *Interfacial Phenomena and Convection* (Chapman and Hall-CRC) 2002.
[8] de Gennes P.-G., *Eur. Phys. J. E*, **6** (2001) 421.
[9] Fanton X. and Cazabat A. M., *Langmuir*, **14** (1998) 2554.
[10] Zhang N. and Chao D. F., *Int. Comm. Heat Mass Transfer*, **26** (1999) 1069.
[11] Maillard M., Motte L., Ngo A. T. and Pileni M. P., *J. Phys. Chem. B*, **104** (2000) 11871.
[12] Sparrow E. M. and Nunez G. A., *Int. J. Heath Mass Transfer*, **31** (1988) 1345.
[13] Saylor J. R., Smith G. B. and Flack K. A., *Phys. Fluids*, **13** (2001) 428.
[14] Fang G. and Ward C. A., *Phys. Rev. E*, **59** (1999) 417; 429; 441.
[15] Bedeaux D. and Kjelstrup S., *Physica A*, **270** (1999) 413.
[16] Marx J. E. (Editor), *Polymer Data Handbook* (Oxford University Press, New York) 1999.
[17] *NIST Chemistry WebBook*, `http://webbook.nist.gov` (2003).
[18] Ondarçuhu T., Millan-Rodriguez J., Mancini H. L., Garcimartín A. and Pérez García C., *Phys. Rev. E*, **48** (1994) 1121.
[19] Eckert K., Bestehorn M. and Thess A., *J. Fluid Mech.*, **356** (1998) 155.
[20] VanHook S. J., Schatz M. F., Swift J. B., McCormick W. D. and Swinney H. L., *Phys. Rev. Lett.*, **75** (1995) 4397.
[21] Merkt D. and Bestehorn M., *Physica D*, **185** (2003) 196.
[22] Pérez García C., Echebarria B. and Bestehorn M., *Phys. Rev. E*, **57** (1998) 475.
[23] Schatz M. F., VanHook S. J., McCormick W. D., Swift J. B. and Swinney H. L., *Phys. Fluids*, **11** (1999) 2577.